GW self-energy calculations for systems with huge supercells

J. Furthmüller,[1] G. Cappellini,[2] H.-Ch. Weissker,[1] and F. Bechstedt[1]
[1]*Institut für Festkörpertheorie und Theoretische Optik, Friedrich-Schiller-Universität, D-07743 Jena, Germany*
[2]*Dipartimento di Fisica, Cittadella Universitaria, S. Prov. le Monserrato-Sestu Km.0.700, I-09042 Monserrato (Cagliari), Italy*
(Received 9 January 2002; published 22 July 2002)

We present parameter-free calculations of the quasiparticle band structure of systems described by huge supercells. They are based on a pseudopotential–plane-wave method to calculate the electronic structure in the ground state. All-electron wave functions are constructed using the projector-augmented wave method. The electronic self-energy is calculated within the GW approximation using an efficient approach to the screening. It includes a simplified treatment of dynamical and local-field effects. The approach is carefully tested by computing the quasiparticle band structure of group-IV semiconductors within nonprimitive unit cells containing 216 atoms. The success of the method is demonstrated by the calculation of the electronic structure of Ge and Si nanocrystallites embedded in a SiC matrix.

DOI: 10.1103/PhysRevB.66.045110 PACS number(s): 71.10.−w, 73.22.−f, 71.45.Gm, 71.15.−m

I. INTRODUCTION

Now parameter-free calculations of systems with huge unit cells containing more than 100 atoms are necessary and possible. Such systems mainly occur due to keeping the three-dimensional translational symmetry in the description of nanosized structures as surfaces, quantum dots, and nanocrystallites. Repeated slabs are used to model surfaces,[1] while clusters of atoms[2,3] are embedded in a supercell which is repeated to form a new artificial crystal. The atomic geometry and the electronic structure are typically described using density-functional theory[4] (DFT) within the local-density approximation (LDA).[5] This is, however, a ground-state theory. The resulting single-particle and two-particle excitation energies do not account for the excitation aspect. Consequently, energy gaps and optical transition energies are considerably underestimated for semiconductors and insulators.[6] A rigorous solution of this electronic excitation problem has been addressed by Hedin's GW approximation to the exchange-correlation self-energy of the electrons.[7]

Applications of the GW theory beginning with the work of Hybertsen and Louie,[8] Godby, Schlüter, and Sham,[9] and other workers have proven very successfully that this scheme works essentially perfectly for a wide range of materials, in particular, for perfect crystals with usually two atoms in the unit cell.[6] However, the GW method requires significant additional computational effort over the DFT LDA because it involves the computation of the dielectric function and the single-particle Green function, and relies on the solution of the Dyson equation, which is more demanding than the single-particle Kohn-Sham equation[5] due to the energy dependence of the self-energy operator. For that reason, there are only very few examples of application of the GW theory to complicated systems such as surfaces[10,11] and clusters.[12] The calculation of the electronic screening requires a restriction to small supercells. In order to extend the calculation to several tens of atoms in the supercell, usually a model dielectric function has been used.[1,13,14]

In this paper, we follow this line. We demonstrate however that quasiparticle band structures can be calculated for supercells containing several hundreds of atoms. In Sec. II the method of electronic-structure calculations based on non-norm-conserving pseudopotentials and the projector-augmented wave method are briefly described. We present the formulas used in the GW approximation. In Sec. III we demonstrate how the method works for supercells with 216 atoms. Resulting excitation energies are compared with those obtained for group-IV semiconductors represented within the primitive two-atom cell. The method is applied to Ge and Si clusters embedded in a cubic SiC matrix. Finally, in Sec. IV a brief summary is given.

II. CALCULATIONAL METHODS

A. Electronic-structure calculations

In a first step we calculate the one-electron states from first principles using DFT within the LDA.[5] The electron-electron interaction is described within the parametrization of Perdew and Zunger.[15] Nonlinear core corrections are taken into account.[16] The interaction of the electrons with the atomic cores is treated by non-norm-conserving *ab initio* Vanderbilt pseudopotentials.[17] They allow a substantial potential softening even for first-row elements.[18] The plane-wave expansion of the eigenfunctions can be restricted by a kinetic-energy cutoff of 19.8 Ry (diamond), 13.2 Ry (SiC), 9.6 Ry (Si), or 8.8 Ry (Ge). We use the Vienna *Ab initio* Simulation Package.[19] It also allows efficient total-energy minimizations. The DFT LDA yields cubic lattice constants $a_0 = 3.531, 4.332, 5.398$, and 5.627 Å and fundamental energy gaps $E_g = 4.15, 1.33, 0.46$, and 0.03 eV for diamond (C), cubic silicon carbide (SiC), silicon (Si), and germanium (Ge). The use of a plane-wave expansion requires a supercell approach for the description of systems without translational symmetry, for instance, a nanocrystallite embedded in a crystalline matrix. We consider an arrangement of simple cubic (sc) cells. The use of the ultrasoft pseudopotentials[18] (US PP) allows to treat extremely large supercells with 512 atoms in the case of a tetrahedrally coordinated bulk.[20] We demonstrate the quasiparticle calculations for sc supercells with 216 atoms. Their edge lengths are 1.1, 1.3, 1.6, and 1.7 nm for C, SiC, Si, and Ge, respectively.

The use of non-norm-conserving pseudopotentials is a disadvantage if explicitly electronic wave functions are needed, for example, to calculate optical transition matrix elements. To solve this problem we apply Blöchl's projector-augmented wave (PAW) approach to the electronic-structure calculation.[21] There is a formal relationship between ultrasoft Vanderbilt-type pseudopotentials and the PAW method.[22] Using projectors onto the core regions of the free atoms and pseudoatoms, all-electron wave functions are constructed for the valence electrons.[23] This approach gives indeed excellent results for the optical transition matrix elements of bulk semiconductors.[23]

B. Quasiparticle shifts

The excitation of a particle, electron, or hole in a Bloch band n at a given wave vector $\mathbf{k}$ in the Brillouin zone (BZ) cannot be described by the eigenvalues $\varepsilon_n(\mathbf{k})$ and eigenfunctions $\Psi_{n\mathbf{k}}(\mathbf{x})$ of the Kohn-Sham equation of the DFT in LDA,[5] since this is a ground-state theory. Instead a quasiparticle equation[8,9] has to be solved. In this equation the local exchange-correlation (XC) potential V_{XC} of the Kohn-Sham theory is replaced by an XC self-energy operator Σ, which is, in general, nonlocal in space, non-Hermitian, and energy dependent. The evaluation of the self-energy operator is a very difficult task. An efficient approximation is the GW scheme,[7,24] in which the self-energy is linearly expanded with respect to the dynamically screened Coulomb potential W. The abbreviation G stands for the one-particle Green function. In the majority of cases, it is sufficient to treat the self-energy effect within first-order perturbation theory. The quasiparticle correction $\Delta_n(\mathbf{k})$ to a Kohn-Sham eigenvalue $\varepsilon_n(\mathbf{k})$ gives the quasiparticle energy $\varepsilon_n^{QP}(\mathbf{k})$. It is defined as

$$\Delta_n(\mathbf{k}) = \langle \Psi_{n\mathbf{k}} | \Sigma(\varepsilon_n^{QP}(\mathbf{k})) - V_{XC} | \Psi_{n\mathbf{k}} \rangle. \tag{1}$$

Because of the smallness of the quasiparticle shift (1), usually a linear expansion of the self-energy around $\varepsilon_n(\mathbf{k})$ is used. This expansion suggests a division of the self-energy into a static contribution Σ^{st} and a part $\Sigma^{dyn}(\varepsilon)$ that is entirely given by the effect of dynamical screening. Usually, in addition the static part Σ^{st} is divided into a Coulomb hole (COH) and a screened exchange (SEX) part,[8,24]

$$\Sigma^{\mathrm{COH}}(\mathbf{x},\mathbf{x}') = \frac{1}{2}\sum_{n,\mathbf{k}} \Psi_{n\mathbf{k}}(\mathbf{x})\Psi^*_{n\mathbf{k}}(\mathbf{x}')[W(\mathbf{x},\mathbf{x}';0) - v(\mathbf{x}-\mathbf{x}')],$$

$$\Sigma^{\mathrm{SEX}}(\mathbf{x},\mathbf{x}') = -\sum_{n,\mathbf{k}}^{\mathrm{occ}} \Psi_{n\mathbf{k}}(\mathbf{x})\Psi^*_{n\mathbf{k}}(\mathbf{x}')W(\mathbf{x},\mathbf{x}';0) \tag{2}$$

with the statically screened Coulomb potential $W(\mathbf{x},\mathbf{x}';0)$ and the bare Coulomb potential $v(\mathbf{x}-\mathbf{x}')$. As a consequence the quasiparticle shift can be written as[6]

$$\Delta_n(\mathbf{k}) = [\Sigma^{\mathrm{COH}}_{n\mathbf{k}} + \Sigma^{\mathrm{SEX}}_{n\mathbf{k}} + \Sigma^{dyn}_{n\mathbf{k}}[\varepsilon_n(\mathbf{k})] - V^{XC}_{n\mathbf{k}}]/[1+\beta_n(\mathbf{k})],$$

$$\beta_n(\mathbf{k}) = -\frac{\partial}{\partial\varepsilon}\Sigma^{dyn}_{n\mathbf{k}}(\varepsilon)\big|_{\varepsilon=\varepsilon_n(\mathbf{k})}. \tag{3}$$

Expression (3) only contains diagonal matrix elements with respect to the Kohn-Sham states $\Psi_{n\mathbf{k}}(\mathbf{x})$.

For small systems, such as bulk crystals with two atoms in the primitive unit cell, the screened potential W is calculated from first principles.[6,8,9] However, the calculation from eigenfunctions and eigenvalues and the inversion of the full dielectric matrix approximately takes 75% of the CPU time needed for the calculation of the quasiparticle correction for a single state.[6] Consequently, this procedure is too time consuming for systems with several hundreds of atoms in the elementary cell. For that reason Bechstedt *et al.*[25] and Cappellini *et al.*[26] suggested to combine the plasmon-pole approximation for the treatment of the dynamics[8] with a model dielectric function. The basic idea is (i) to treat the local-field effects by an inverse dielectric function $\epsilon^{-1}(\mathbf{q},0;n(\mathbf{x}))$ depending on the actual electron density and (ii) to replace this quantity by state-averaged values. This allows a simplified representation of all contributions to the shift (3). The SEX term can be written as[27]

$$\Sigma^{\mathrm{SEX}}_{n\mathbf{k}} = -\frac{4\pi e^2}{V}\sum_{n'}^{\mathrm{occ}}\Bigg\{\sum_{\mathbf{k}'}\sum_{\mathbf{G}(\neq 0)}|\Gamma_{n\mathbf{k},n'\mathbf{k}'}(\mathbf{G})|^2 \times\frac{\epsilon^{-1}(\mathbf{k}-\mathbf{k}'+\mathbf{G},0)}{|\mathbf{k}-\mathbf{k}'+\mathbf{G}|^2} + \sum_{\mathbf{k}'(\neq\mathbf{k})}|\Gamma_{n\mathbf{k},n'\mathbf{k}'}(0)|^2 \times\frac{\epsilon^{-1}(\mathbf{k}-\mathbf{k}',0)}{|\mathbf{k}-\mathbf{k}'|^2} + \delta_{nn'}\Sigma^{\mathrm{SEX}}_n(0)\Bigg\} \tag{4}$$

with V as the volume of the system and $\Sigma^{\mathrm{SEX}}_n(0)$ the contribution related to the Coulomb singularity in $\mathbf{k}$ space. In expression (4) Fourier transforms of products of Bloch functions

$$\Gamma_{n\mathbf{k},n'\mathbf{k}'}(\mathbf{x}) = \Psi_{n\mathbf{k}}(\mathbf{x})\Psi^*_{n'\mathbf{k}'}(\mathbf{x}) = \sum_{\mathbf{G}} e^{i(\mathbf{k}-\mathbf{k}'+\mathbf{G})\mathbf{x}}\Gamma_{n\mathbf{k},n'\mathbf{k}'}(\mathbf{G}) \tag{5}$$

occur. Meanwhile, the validity of the approximations (3) and (4) has been tested by application to common semiconductors,[25,26] wide-band-gap semiconductors,[27–29] and insulating charge-transfer oxides[30] as well as semiconductor surfaces.[14] Efficient self-energy calculations can be thus carried out on common workstations.

C. Computational details

The inverse dielectric function ϵ^{-1} used in the self-energy calculations[26] does not only depend on the electron density $n(\mathbf{x})$ directly obtained from the DFT-LDA treatment of the electronic system. It is also influenced by the electronic di-

electric constant ϵ_∞. For well-known materials this value can be taken from experiment. However, for unknown systems, e.g., systems consisting of embedded nanocrystals, the dielectric constant has to be calculated. We do this within the independent-particle approximation.[31] For vanishing frequency and wave vector, ϵ_∞ follows directly from the Ehrenreich-Cohen formula and the Kohn-Sham eigenvalues and eigenfunctions. Since local-field effects are not included, we compute $\epsilon_\infty = 13.755$ for bulk Si. This value is somewhat larger than the experimental value $\epsilon_\infty = 11.3$. We checked the effect of the variation of the dielectric constant on the quasiparticle shifts of four occupied and empty bands around the fundamental gap at the Γ and X points of the BZ. Typical variations due to the different dielectric constants are smaller than 50 meV. In the case of the lowest valence-band state at Γ we found the strongest variation to be 85 meV. Consequently, in the following we use the dielectric constants calculated within the independent-particle approximation.

The evaluation of the quasiparticle corrections (3) to the DFT-LDA band structures, especially of the SEX contribution (4), needs to be done with some care due to the presence of an integrable divergence. A reduction of the numerical effort by using a limited number of **k** points in the irreducible part of the BZ is possible applying the method proposed by Gygi and Baldereschi.[32] An analytical function possessing the Coulomb singularity in **k** space is introduced. One calculates the integral over this function and substracts the resulting approximate value from the exact integral $\Sigma_n^{\mathrm{SEX}}(0)$ in expression (4). Since an integral over the BZ has to be performed, the Gygi-Baldereschi procedure is related to two numerical disadvantages. For each Bravais-lattice type another auxiliary function has to be chosen, and no improvement of the **k**-sampling quality occurs for large supercells. For that reason, we use another procedure. A Gaussian multiplied with the Fourier-transformed Coulomb potential is introduced. The advantages are that, since the integral over the entire space can be carried out analytically, this procedure can be used for all crystal structures, and systematic improvements of the **k**-sampling quality are possible.

The products of Bloch wave functions (5) in the SEX term (4) can be divided into a contribution from the non-norm-conserving pseudowave functions and an augmentation contribution inside the core regions localized at atomic sites **R**.[21,23] One finds

$$\Gamma_{n\mathbf{k},n'\mathbf{k}'}(\mathbf{x}) = \tilde{\Psi}_{n\mathbf{k}}(\mathbf{x})\tilde{\Psi}^*_{n'\mathbf{k}'}(\mathbf{x}) + \sum_{\mathbf{R}} \sum_{i,i'} P_{i\mathbf{R},n\mathbf{k}} P^*_{i'\mathbf{R},n'\mathbf{k}'} \times [\Phi_{i\mathbf{R}}(\mathbf{x})\Phi^*_{i'\mathbf{R}}(\mathbf{x}) - \tilde{\Phi}_{i\mathbf{R}}(\mathbf{x})\tilde{\Phi}^*_{i'\mathbf{R}}(\mathbf{x})], \quad (6)$$

$$P_{i\mathbf{R},n\mathbf{k}} = \langle \tilde{p}_{i\mathbf{R}} | \tilde{\Psi}_{n\mathbf{k}} \rangle$$

with $\tilde{\Psi}_{n\mathbf{k}}(\mathbf{x})$ as the non-norm-conserving pseudowave functions. The index i is a shorthand for the angular momentum quantum numbers and the reference energies at which we construct the atomic pseudopartial waves $\tilde{\Phi}_{i\mathbf{R}}(\mathbf{x})$. The quantities $\Phi_{i\mathbf{R}}(\mathbf{x})$ are either norm-conserving atomic pseudowave functions in the US-PP case or all-electron wave functions in the PAW case. The quantities $[\Phi_{i\mathbf{R}}(\mathbf{x})\Phi^*_{i'\mathbf{R}}(\mathbf{x}) - \tilde{\Phi}_{i\mathbf{R}}(\mathbf{x})\tilde{\Phi}^*_{i'\mathbf{R}}(\mathbf{x})]$ correspond to the atomic augmentation charges also used for the augmentation of the total charge density. Hence, the implementation of expression (6) is straightforward even in the US-PP case. In the PAW case an extra complication arises since a proper all-electron augmentation requires an extra logarithmic radial support mesh within the core region of each atom. In order to limit the numerical effort we restrict ourselves to a norm-conserving pseudoaugmentation charge also in the PAW case. Although this procedure is not exact, the numerical errors introduced are negligible. The pseudopartial waves are usually non-norm-conserving as in the Vanderbilt pseudopotential scheme.[17–19] The projectors $|\tilde{p}_{i\mathbf{R}}\rangle$ introduced in the definition (6) of $P_{i\mathbf{R},n\mathbf{k}}$ are dual to the pseudopartial waves, i.e., $\langle \tilde{p}_{i\mathbf{R}} | \tilde{\Phi}_{i'\mathbf{R}'} \rangle = \delta_{ii'}\delta_{\mathbf{R}\mathbf{R}'}$. Inside an augmentation sphere the completeness relation $\Sigma_i |\tilde{\Phi}_{i\mathbf{R}}\rangle\langle \tilde{p}_{i\mathbf{R}}| = 1$ holds.

The computational effort of the Fourier transforms of the product (6) depends on the density of the real-space mesh. In the case of the DFT-LDA calculations we use for two-atom cells of the bulk crystals under consideration a $16\times16\times16$ mesh for the wave functions and a $24\times24\times24$ mesh for the augmentation charge density. Test calculations for Si showed that the SEX contribution to the self-energy is rather insensitive to extreme reductions of the mesh size. Even for a huge 216-atom supercell a $30\times30\times30$ mesh is sufficient. Another limiting quantity is the density of the **k** points in the BZ integration. We use special points of the Monkhorst-Pack (MP) type.[33] With the novel treatment of the Coulomb singularity we found convergence already for $4\times4\times4$ samplings with an accuracy of about 1 meV for the total quasiparticle shift of states in a Si crystal studied in two-atom cells. Consequently, we use a $2\times2\times2$ MP mesh for sc 216-atom cells. In order to keep the numerical effort as small as possible we restrict ourselves to the $\mathbf{k}'$ points in that irreducible part of the BZ corresponding to the common minimum little group of all **k** points. However, doing this a resymmetrization of the quasiparticle shifts of initially degenerate electronic levels becomes necessary via an averaging of the shifts calculated for all members of a group of degenerate states. In our implementation the energetical degeneracy is detected empirically by comparison of the DFT-LDA eigenvalues. This works very reliably as long as too large artificial symmetry breakings due to insufficient numerical accuracy do not occur and as long as the spectrum of eigenvalues becomes not so extremely dense that nearly degenerate and truly degenerate states cannot be distinguished anymore. With the real-space and **k**-space meshes mentioned for a system with 216-atom elementary cells the quasiparticle calculation can be done for one **k** point and one $\mathbf{k}'$ point in 30–40 hours using a common workstation. That means that the DFT-LDA calculation for a 216-atom cell is still more time consuming than the computation of the GW corrections within our method.

III. RESULTS AND DISCUSSION

A. GW approximation: 216-atom versus two-atom cells

In order to test the GW scheme described in Sec. II B for large-supercell systems, we study the diamond-structure

TABLE I. Single-particle energies for Si bulk in DFT-LDA and quasiparticle (QP) approximation. Quasiparticle shifts and contributions to the self-energy are listed. All values are in eV, with the exception of the dimensionless satellite strength $\beta_n(\mathbf{k})$. The quantities are calculated within two-atom cells and 216-atom cells (in parentheses, where deviating).

Band state	$\varepsilon_n(\mathbf{k})$	$\Sigma_{n\mathbf{k}}^{\mathrm{COH}}$	$\Sigma_{n\mathbf{k}}^{\mathrm{SEX}}$	$\Sigma_{n\mathbf{k}}^{dyn}$	$V_{n\mathbf{k}}^{XC}$	$\beta_n(\mathbf{k})$	$\Delta_n(\mathbf{k})$	$\varepsilon_n^{QP}(\mathbf{k})$
Γ_{1v}	−12.082	−8.712	−4.877	1.762	−10.517	0.248	−1.049	−12.893
			(−4.870)				(−1.044)	(−12.887)
$\Gamma_{25'v}$	0	−9.197	−4.229	1.829	−11.303	0.236	−0.239	0
			(−4.229)				(−0.239)	
Γ_{15c}	2.529	−8.468	−2.789	1.713	−10.104	0.258	0.445	3.213
			(−2.787)				(0.446)	(3.214)
$\Gamma_{2'c}$	3.347	−8.986	−3.144	1.794	−10.952	0.242	0.496	4.082
			(−3.131)				(0.507)	(4.093)
X_{1v}	−7.888	−8.934	−4.677	1.790	−10.871	0.243	−0.764	−8.413
			(−4.671)				(−0.760)	(−8.409)
X_{4v}	−2.913	−8.779	−4.033	1.769	−10.621	0.247	−0.338	−3.012
			(−4.034)				(−0.338)	(−3.012)
X_{1c}	0.578	−7.859	−2.428	1.637	−9.165	0.275	0.404	1.221
			(−2.426)				(0.405)	(1.223)

crystal Si. The primitive cell of the fcc crystal contains two Si atoms. In addition, we describe this material in a nonprimitive sc cell with 216 atoms. For folding reasons the electronic structure is only studied at the Γ and X points of the fcc BZ. The most important band states are considered. They are the valence bands Γ_1,$\Gamma_{25'}$,X_1, and X_4. In the case of the conduction bands we consider the states X_1,Γ_{15}, and $\Gamma_{2'}$. The results are presented in Table I. The data computed for the two different cells are practically identical. Only a tiny variation of the SEX term of few meV occurs as a consequence of the different real-space and **k**-space meshes. In particular the extreme reduction of the real-space meshes is responsible for the major fraction of the total error. However, this variation is small compared to the accuracy of the quasiparticle energies of about 0.1 eV. The question arises whether this agreement is still valid for crystals with stronger or even ionic bonds. For diamond we observe a small increase of the deviations to a maximum value of 0.03 eV. For SiC this deviation even increases. The largest variations of the SEX term occur for Γ_{15c} with $-6.988(-7.077)$ eV or for X_{1c} with $-3.295(-3.162)$ eV in two-atom (216-atom) cells. This results in a maximum variation of the quasiparticle energies by about 0.08 eV. We conclude that the simplified self-energy calculation described in Sec. II B can be performed in small and huge unit cells with the same accuracy.

The quality of the self-energy calculations within 216-atom cells and the simplified GW scheme becomes obvious by the comparison with results of other calculations using two-atom cells and a more accurate screening[8,34] as well as with experimental data[8,35,36] in Table II. The quasiparticle shifts are calculated using the computed values ϵ_∞

TABLE II. Quasiparticle energies of important band states with respect to the Γ_{25}' valence-band maximum (in eV). For comparison the Kohn-Sham (KS) values from the DFT LDA are also given. The values are compared with previous theoretical and experimental results (exp.) (second column) (Refs. 8 and 34–36).

Crystal	Method	Indirect gap		Direct gap		Valence bandwidth	
Diamond	KS	4.19	3.9	5.62	5.5	21.69	21.6
	QP	5.66	5.6	7.42	7.5	24.07	23.0
	exp.		5.48		7.3		24.2±1,21±1
SiC	KS	1.34	1.22	6.56	6.57	15.44	15.07
	QP	2.57	2.37	7.90	7.81	16.85	16.13
	exp.		2.42		7.4		
Si	KS	0.44	0.52	2.43	2.57	12.08	11.93
	QP	1.06	1.29	3.21	3.35	12.89	12.04
	exp.		1.17		3.4		12.5±0.6
Ge	KS	0.12	0.07	0.03		12.91	
	QP	0.57	0.75	0.45	0.71	13.71	12.86
	exp.		0.774		0.89		12.6, 12.9±0.2

TABLE III. Kohn-Sham and quasiparticle energies at Γ of the lowest empty ($n \geqslant 433$) and highest occupied ($\leqslant 432$) bands of the composite material with supercells of 17 Ge, 95 Si, and 104 C atoms. All values are in eV.

n	$\varepsilon_n(0)$	$\varepsilon_n^{QP}(0)$
438–440	11.020	11.732
436–437	10.989	11.699
433–434	9.786	10.421
432–430	8.860	8.431
429–427	8.243	7.711
425–426	8.215	7.697

$=5.864,7.132$, and 13.755 for C, SiC, and Si. For the critical case of Ge with its practically vanishing gap and hence almost infinite calculated ϵ_∞ we use a value $\epsilon_\infty = 16$ reflecting approximately the room-temperature experimental value. The overall agreement for the energy gaps is excellent. The deviations approach the predicted accuracy of about 0.1 eV. Only in the Ge case do our calculations underestimate the gaps. However, this is more a consequence of the overestimation of the repulsion between Ge 3*d* and Ge 4*p* states. The simplified GW treatment tends to overestimate the QP shift of states far away from the fundamental gap, e.g., of Γ_{1v}. Perhaps, this tendency results in a tiny overestimation of the valence-band widths. Altogether, we can again conclude that the method developed in Sec. II allows reliable quasiparticle calculations for systems with several hundreds of atoms in the unit cell.

B. Quasiparticle bands of a composite: Ge and Si nanocrystals in a SiC matrix

Recently composite systems with very interesting optoelectronic properties have been prepared. Self-assembled germanium nanocrystallites have been grown on a SiC(0001) surface during a molecular-beam deposition.[37] Ion implantation with subsequent annealing yields Ge or mixed GeSi nanocrystallites in a hexagonal SiC matrix.[38] The band structures and the accompanying optical properties of such systems are completely unknown. A first step of the understanding of these systems could be the calculation of the quasiparticle band structure. In order to perform such a calculation we study sc 216-atom supercells filled with cubic SiC. The Si and C atoms at atomic sites in the center of each supercell are replaced by 17 Ge or Si atoms. The atomic structure is assumed to remain unchanged, i.e., the atoms keep the tetrahedral coordination and all bonds in the interface between nanocrystallite and host are saturated. The clusters possess nearly spherical symmetry. The point group of the supercell system is still T_d. The resulting Ge (Si) nanocrystallites are highly strained due to the large lattice misfit. We study only systems with Ge-C (Si-C) interface bonds.

An effective dielectric constant $\epsilon_\infty = 8.0$ (7.5) is computed for the Ge/SiC (Si/SiC) composite system. To illustrate the quasiparticle effect the Kohn-Sham and quasiparticle eigenvalues of the highest occupied supercell bands and the lowest empty bands are listed in Table III for the Ge nanocrystallite in 3C-SiC. Resulting band structures are presented in Figs. 1 and 2 for two different approximations. In Figs. 1(a) and 2(a) the Kohn-Sham eigenvalues are plotted, whereas in Figs. 1(b) and 2(b) the GW quasiparticle corrections (3) are added. The alignment between the DFT-LDA band structures (and in a similar procedure of the GW band structures) of the pure SiC bulk and the composite system has been made using characteristic SiC-related contributions to the densities of states. Those of the composite systems are plotted in Fig. 3 in the energy range of the highest occupied and lowest unoccupied states. Independent of the treatment of the many-body effects, the Ge nanocrystallites induce occupied electronic states in the fundamental gap of cubic SiC near the valence-band maximum. The bound states in the gap can be interpreted as hole levels, the wave functions of which are localized in the central Ge cluster. The quasiparticle effects leave the energy region around the valence-band maximum (VBM) of SiC and the occupied Ge-induced states

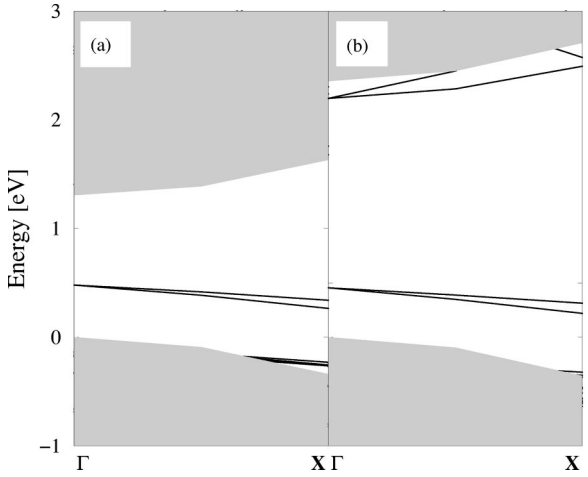

FIG. 1. Projected bulk SiC band structure (shaded area) and Ge-induced gap states (solid lines) of a 17-atom Ge cluster embedded in a cubic SiC matrix. Supercells of 216 atoms and the ΓX line in the corresponding BZ are considered. (a) DFT-LDA bands; (b) GW quasiparticle bands. The valence-band maximum of SiC is used as zero energy.

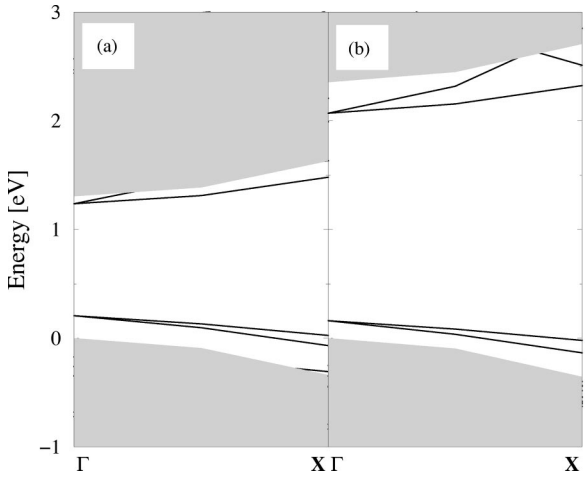

FIG. 2. As in Fig. 1 but for a Si nanocrystallite.

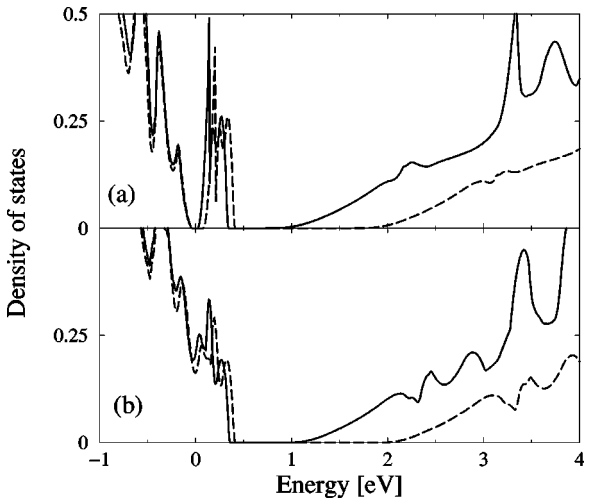

FIG. 3. Electronic density of states without (dashed line) and with (solid line) quasiparticle effects for 17-atom nanocrystallites in SiC. (a) Ge; (b) Si.

within the fundamental gap practically unchanged. Within the DFT LDA the lowest electron states are built up by wave functions of the SiC system. The composite system consisting of Ge and SiC can therefore be interpreted as a type-II heterostructure with a staggered alignment of the conduction- and valence-band edges.[39] This finding is in agreement with the positions of the valence-band edges derived within a tight-binding theory[40] and using the experimental energy gaps given in Table II. With quasiparticle effects [see Fig. 1(b)] supercell bands appear close to the conduction-band edge of SiC. This seems to be a consequence of the fact that in the composite system with Ge atoms the electronic screening is slightly less effective in comparison to that of the pure SiC system. The wave functions of these supercell states remain strongly delocalized. Consequently, the type-II heterostructure is conserved taking the excitation aspect into account.

Interestingly the quasiparticle shifts in Table III do not strongly vary with their character as states localized in the Ge nanocrystals or bulklike SiC states. This is mainly a consequence of the joint screening function of the composite that is used for all states. The main influence of the quasiparticle effects results in a widening of the fundamental energy gap of the SiC host. The dispersion of the bands, on the other hand, remains widely unchanged. This is clearly demonstrated by the density of states in Fig. 3 for the Ge but also for the Si nanocrystal embedded in a SiC matrix. Much more than in the band structures the influence in the fundamental gap region seems to be characterizable by a rigid shift of the empty states with respect to the occupied states.

The behavior of the electronic states of the composite system consisting of a Si nanocrystal embedded in a SiC matrix is very similar to that of the Ge/SiC case (see Fig. 2). There are, however, two differences. The Si-induced occupied states are closer to the VBM of SiC, and unoccupied states appear close to the SiC conduction-band edge already within the DFT-LDA approach. The corresponding wave functions are weakly localized in the Si nanocrystal. Therefore, the composite system of highly strained Si crystallites embedded in a SiC matrix tends to a type-I heterostructure system. As in the Ge case (see Fig. 1) this tendency is strengthened within the GW approach.

IV. SUMMARY

Summarizing, a quasiparticle computational scheme has been developed that is applicable to nonmetallic systems with large unit cells containing several hundreds of atoms. This scheme represents a generalization of an efficient GW method for the evaluation of the first-order quasiparticle corrections to the electronic band structure obtained within DFT LDA. The screening function of the system is replaced by a model function. Aside from this model the theory remains parameter-free. The electronic charge density and the electronic dielectric constant, which governs the screening of the Coulomb interaction, are taken from an independent-particle calculation within the DFT-LDA.

In order to determine the structure and the electronic states of systems with huge unit cells (>200 atoms), in particular, when first-row elements are involved, non-norm-conserving pseudopotentials are used to describe the electron-ion interaction. The corresponding electronic-structure calculations do not give an orthonormalized and complete set of wave functions in the entire space. However, since only the atomic augmentation charges are needed and no real full reconstruction of wave functions is necessary, it is straightforward to implement the matrix elements of the self-energy operator even in the US-PP case. Nevertheless, considering the strict similarities between the PAW method and the ultrasoft non-norm-conserving pseudopotentials it is also possible to use the PAW approach. The PAW method allows the construction of all-electron wave functions for the valence electrons. This becomes important if one likes to combine the calculation of optical properties with the calculation of quasiparticle energies.

The method developed as well as the numerical approaches are tested by calculating the quasiparticle bands for the stable group-IV crystals diamond, SiC, Si, and Ge. We show that when using nonprimitive cells with 216 atoms the same quasiparticle shifts are obtained as in the limit of primitive two-atom cells. The efficiency of the method has been demonstrated for composite systems. We studied Ge and Si nanocrystallites embedded in cubic SiC.

ACKNOWLEDGMENTS

We acknowledge financial support from the Deutsche Forschungsgemeinschaft (Sonderforschungsbereich 196, Project No. A8) and the European community within a research training network (Contract No. HPRN-CT-2000-00167). Part of the numerical calculations has been done using the facilities of the J. v. Neumann Institute for Computing in Jülich. G. Cappellini would like to thank Luciano Colombo for many useful discussions.

[1] W.G. Schmidt, J.L. Fattebert, J. Bernholc, and F. Bechstedt, Surf. Rev. Lett. **6**, 1159 (1999).
[2] G. Onida, L. Reining, R.W. Godby, R. Del Sole, and W. Andreoni, Phys. Rev. Lett. **75**, 818 (1995).
[3] H.-Ch. Weissker, J. Furthmüller, and F. Bechstedt, Phys. Status Solidi B **224**, 769 (2001); Mater. Sci. Forum **353-356**, 413 (2001).
[4] P. Hohenberg and W. Kohn, Phys. Rev. **136**, B864 (1964).
[5] W. Kohn and L.J. Sham, Phys. Rev. **140**, A1133 (1965).
[6] F. Bechstedt, Adv. Solid State Phys. **32**, 161 (1992).
[7] L. Hedin, Phys. Rev. **139**, A796 (1965).
[8] M.S. Hybertsen and S.G. Louie, Phys. Rev. B **34**, 5390 (1986).
[9] R.W. Godby, M. Schlüter, and L.J. Sham, Phys. Rev. B **37**, 10 159 (1988).
[10] M. Rohlfing, P. Krüger, and J. Pollmann, Phys. Rev. B **52**, 1905 (1995).
[11] O. Pulci, G. Onida, R. Del Sole, and L. Reining, Phys. Rev. Lett. **81**, 5374 (1998).
[12] L. Reining, O. Pulci, M. Palummo, and G. Onida, Int. J. Quantum Chem. **77**, 951 (2000).
[13] J.E. Northrup, Phys. Rev. B **47**, 10 032 (1993).
[14] P.H. Hahn, W.G. Schmidt, and F. Bechstedt, Phys. Rev. Lett. **88**, 016402 (2002).
[15] J.P. Perdew and A. Zunger, Phys. Rev. B **23**, 5048 (1981).
[16] S.G. Louie, S. Froyen, and M.L. Cohen, Phys. Rev. B **26**, 1738 (1982).
[17] D. Vanderbilt, Phys. Rev. B **41**, 7892 (1990).
[18] J. Furthmüller, P. Käckell, F. Bechstedt, and G. Kresse, Phys. Rev. B **61**, 4576 (2000).
[19] G. Kresse and J. Furthmüller, Comput. Mater. Sci. **6**, 15 (1996); Phys. Rev. B **54**, 11 169 (1996).
[20] H.-C. Weissker, J. Furthmüller, and F. Bechstedt, Phys. Rev. B **64**, 035105 (2001).
[21] P.E. Blöchl, Phys. Rev. B **50**, 17 953 (1994).
[22] G. Kresse and D. Joubert, Phys. Rev. B **59**, 1758 (1999).
[23] B. Adolph, J. Furthmüller, and F. Bechstedt, Phys. Rev. B **63**, 125108 (2001).
[24] L. Hedin and S. Lundqvist, Solid State Phys. **23**, 1 (1969).
[25] F. Bechstedt, R. Del Sole, G. Cappellini, and L. Reining, Solid State Commun. **84**, 765 (1992).
[26] G. Cappellini, R. Del Sole, L. Reining, and F. Bechstedt, Phys. Rev. B **47**, 9892 (1993).
[27] B. Wenzien, G. Cappellini, and F. Bechstedt, Phys. Rev. B **51**, 14 701 (1995).
[28] M. Palummo, R. Del Sole, L. Reining, F. Bechstedt, and G. Cappellini, Solid State Commun. **95**, 393 (1995).
[29] B. Wenzien, P. Käckell, F. Bechstedt, and G. Cappellini, Phys. Rev. B **52**, 10 897 (1995).
[30] G. Cappellini, S. Bouette-Russo, B. Amadon, C. Noguera, and F. Finocchi, J. Phys.: Condens. Matter **12**, 3671 (2000).
[31] B. Adolph, V.I. Gavrilenko, K. Tenelsen, F. Bechstedt, and R. Del Sole, Phys. Rev. B **53**, 9797 (1996).
[32] F. Gygi and A. Baldereschi, Phys. Rev. B **34**, 4405 (1986).
[33] H.J. Monkhorst and J.D. Pack, Phys. Rev. B **13**, 5188 (1976).
[34] W.H. Backes, P.A. Bobbert, and W. van Haeringen, Phys. Rev. B **51**, 4950 (1995).
[35] R.G. Humphreys, D. Bimberg, and W.J. Choyke, Solid State Commun. **39**, 163 (1981).
[36] W.R.L. Lambrecht, B. Segall, M. Yoganathan, W. Suttrop, R.P. Devaty, W.J. Choyke, J.A. Edmond, J.A. Powell, and M. Alouani, Phys. Rev. B **50**, 10 722 (1994).
[37] B. Schröter, K. Komlev, U. Kaiser, G. Hess, G. Kipshidze, and W. Richter, Mater. Sci. Forum **353-356**, 247 (2001).
[38] Ch. Schubert, U. Kaiser, A. Hedler, W. Wesch, T. Gorelik, U. Glatzel, J. Kräusslich, B. Wunderlich, G. Hess, and K. Goetz, J. Appl. Phys. **91**, 1520 (2002).
[39] F. Bechstedt and R. Enderlein, *Semiconductor Surfaces and Interfaces* (Akademie-Verlag, Berlin 1988).
[40] W. A. Harrison, *Electronic Structure and the Properties of Solids* (Dover, New York, 1989).